RSC Pharmaceutics

ROYAL SOCIETY OF CHEMISTRY

PAPER

View Article Online
View Journal

Cite this: DOI: 10.1039/d6pm00089d

Design and development of niacinamide lipid and polymeric nanoparticles and *in vitro* permeation studies using human epidermis

Dimitra Bompou,[a] Emanuela Di Biase,[b] Alexandra Sarika,[a] Efstathia Triantafyllopoulou,[a] Natassa Pippa, *[a] Dimitrios M. Rekkas[a] and Paraskevas P. Dallas*[a]

Niacinamide (NIAC), also known as nicotinamide, is a Biopharmaceutics Classification System (BCS) Class I compound with versatile known dermatological benefits, including anti-inflammatory, antioxidant, brightening, and skin barrier-restoring effects. However, due to its high hydrophilicity and the barrier properties of the stratum corneum, it is characterized by poor skin permeation. This study aimed to develop both lipid and polymer nanoparticles and comparatively assess their potential for the enhancement of NIAC delivery through the skin. Lipid nanoparticles composed of hydrogenated soy phosphatidylcholine (HSPC) and phosphatidylglycerol (PG) were prepared *via* a simple thin-film hydration method. A two-factor (3^2) factorial experimental design was used to determine the effects of PG and colloidal concentration (CollC) on physicochemical properties: hydrodynamic diameter (D_h), polydispersity index (PDI), zeta potential, and encapsulation efficiency (EE) of NIAC, as well as to optimize the lipid formulation. The presence of PG ameliorated physicochemical characteristics and increased NIAC encapsulation up to 56%. Two of five optimized formulations were further investigated for *in vitro* permeation across human epidermis using Franz diffusion cells, with a non-optimized formulation and a 4.5% NIAC solution used as references. Optimized LNPs substantially enhanced skin permeation; compared with the non-optimized formulation, they improved permeation by 39% and overall delivery by 22%. Compared with the 4.5% NIAC solution, they exhibited 192% greater permeation and 800% higher overall delivery efficiency. These findings demonstrate the potential of PG-containing LNPs as effective nanocarriers for cosmetic or dermatological applications. In parallel, polymeric nanoparticles based on Kolliphor® P407 were prepared by bath sonication as an alternative delivery platform for niacinamide, where the influence of the polymer and compound concentrations was examined. Interestingly, the formulation with the minimum total concentration (10 mg mL^{-1}, 9 : 1 polymer : NIAC ratio) displayed the best overall performance, achieving a balance of colloidal stability, micellar homogeneity, and release capacity. Overall, polymeric nanoparticles yielded interesting delivery profiles for the hydrophilic molecule and appeared to facilitate its permeation through the skin, despite the rather limited NIAC encapsulation efficiency achieved; their potential remains to be elucidated more extensively.

Received 7th March 2026,
Accepted 22nd May 2026

DOI: 10.1039/d6pm00089d

rsc.li/RSCPharma

Introduction

Niacinamide (NIAC—molecular formula: $C_6H_6N_2O$), also known as nicotinamide, is an amide form of vitamin B_3 with a $pK_a \approx 3.3$ at 20 °C. It is a water-soluble compound that has a crucial role in the synthesis of nicotinamide adenine dinucleotide, a pyridine nucleotide that serves as a cofactor for the synthesis of NADH and NADPH. These coenzymes are essential in redox reactions and energy generation processes in mammalian cells.[1,2] It is a well-tolerated ingredient of cosmetic products, with extensively studied dermal administration and topical effects. It is shown to improve many skin conditions, such as acne vulgaris, melasma, atopic dermatitis, rosacea, and psoriasis. In recent years it has gained popularity as an anti-aging agent, and it has been shown to improve skin's elasticity and reduce oxidative stress and inflammation.[3,4] It has also been proven effective at restoring skin barrier function, as it increases biosynthesis of sphingolipids, including ceramides and other stratum corneum lipids.[5,6]

[a]*Section of Pharmaceutical Technology, Department of Pharmacy, School of Health Sciences, National and Kapodistrian University of Athens (NKUA), Panepistimioupolis Zografou, 15771 Athens, Greece.*
E-mail: natpippa@pharm.uoa.gr, dallas@pharm.uoa.gr
[b]*Department of Pharmaceutical Sciences, University of Perugia, via del Liceo 1, 06123 Perugia, Italy*

The stratum corneum is the outermost layer of the skin and serves as a main barrier to drug penetration. It consists of a layer of dead keratinized cells with an intercellular matrix, mainly of ceramides, cholesterol, and free fatty acids.[7,8] Niacinamide has a low molecular weight (122.13 g mol^{-1}); however, since it is a BCS I drug with high aqueous solubility (1 g mL^{-1}), it has poor skin permeability; therefore, the development of new formulations to overcome this obstacle is essential.[9,10]

Recently nanocarriers, and more specifically lipid nanoparticles (LNPs), have attracted the interest of the research community as an attempt to develop more versatile drug delivery platforms. LNPs are composed of biocompatible lipids that can form self-assembled structures in aqueous environments. These structures enable the encapsulation of therapeutic or diagnostic compounds within an aqueous core or lipid matrix, depending on their physicochemical properties.[11,12]

Encapsulation protects drugs from *in vivo* degradation, enhances solubility and bioavailability, enables targeted or controlled delivery, and thereby overcomes key limitations of conventional drug-delivery systems.[13] By carrying both hydrophilic and hydrophobic drugs, LNPs may improve skin permeability of niacinamide, reduce required dosage, lower formulation costs, and minimize adverse effects.[14,15] In fact, various nanocarriers have been designed to address NIAC's skin delivery, namely liposomes and solid lipid nanoparticles.[14,16–18]

Besides lipid-based nanocarriers, polymer-based nanocarriers have surfaced as highly promising platforms due to their intrinsic qualities, including safety, stability, solubility, tunable physicochemical characteristics, biocompatibility, and biodegradability.[19] Polymer-based nanoparticles provide strong protection for the encapsulated cargos, increase systemic circulation, enable controlled and targeted release, and enhance cellular uptake efficiency.[19,20] Their favorable solubility, stability, and capacity for sustained release further contribute to enhanced drug absorption, protection from premature degradation, and ameliorated bioavailability.[20] Polymer-based nanoparticles can be synthesized from both natural and synthetic polymers, with the possibility of engineering their molecular weights and structures to optimize encapsulation efficiency and release kinetics.[21] Moreover, surface functionalization with targeting ligands enables site-specific delivery, while the incorporation of stimuli-responsive elements (*e.g.*, pH or temperature sensitivity) allows spatiotemporally controlled drug release. These attributes position polymer-based nanoparticles as versatile and adaptable tools for precision drug therapy and advanced biomedical applications.[21]

The quality of a pharmaceutical and cosmetic product must be built into its design to ensure its safety and efficacy. Traditional approaches such as Quality by Testing (QbT) are considered insufficient and inadequate practices; instead, Quality by Design (QbD) was suggested by the regulatory authorities (FDA, EMA) at the beginning of the new millennium, emphasizing that quality should be part of product development.[22,23]

Design of Experiments (DOE) represents a core element of QbD, which was introduced in the 20th century by statistician Sir Ronald Fisher, who first emphasized the importance of applying statistical methodology early in a process. DoE provides a systematic approach for determination, optimization, and control of both formulation and process parameters. During the development of a formulation, where multiple variables are involved, it enables the study of the effect of each individual factor and their interactions, the identification of critical variables, and supports optimization through careful selection of their levels.[24–26]

The aim of this study was the formulation of 1% niacinamide in lipid nanoparticles composed of hydrogenated soy phosphatidylcholine (HSPC) and phosphatidylglycerol (PG). Several saturated phosphatidylcholines can be used for the preparation of lipid nanoparticulate drug delivery systems as penetration enhancers for dermal and transdermal applications. Lipid composition is critical for the colloidal stability, drug loading, and release behavior of the final formulation. The main transition temperature governs their behavior and the critical process parameters (CPPs) as well. Dipalmitoylphosphatidylcholine (DPPC), distearoylphosphatidylcholine (DSPC), and HSPC are the most common lipids in the marketed available nanomedicines.[27] HSPC is a widely used, saturated, zwitterionic phospholipid featured in several approved formulations, while PG is an anionic phospholipid whose incorporation can modulate the surface charge, bilayer packing, and colloidal stability of the nanoparticles. The HSPC was used due to its high degree of biocompatibility and its well-established behavior in preclinical, clinical, and post-market vigilance studies. To the best of our knowledge, this is the first time that the use of PG lipid is evaluated for the enhancement of NIAC skin permeation.

The lipid nanoparticles were prepared by the thin film hydration method, followed by bath sonication to reduce their size. Design of Experiments (DoE) was used as a statistical tool for the optimization of the relationship between the variables and the responses, specifically to determine the appropriate amount of PG and the colloidal concentration, within their respective ranges, that result in a formulation with minimum D_h, PDI, and zeta potential, while maximizing the encapsulation efficiency of niacinamide. In addition, pure nanocarriers were prepared, characterized, and compared to the 1% NIAC-loaded nanocarriers.

In parallel, polymeric nanoparticles based on Kolliphor® P407 were manufactured *via* bath sonication in order to provide a comparative evaluation between lipid- and polymer-based nanocarriers for the skin delivery of a highly hydrophilic molecule such as niacinamide. More specifically, niacinamide-loaded formulations were prepared at three different polymer concentrations (10 mg mL^{-1}, 20 mg mL^{-1}, and 30 mg mL^{-1}, respectively) with a polymer-to-drug ratio of 9 : 1 to examine the effect of polymer and NIAC concentration on the physicochemical properties of the polymeric nanoparticles and their release performance. Similarly to lipid-based nanocarriers, pure polymeric nanoparticles at the same polymer concen-

trations were also prepared. Finally, for both lipid and polymeric nanoparticles, an *in vitro* skin permeation study (IVPT) was conducted using a Franz diffusion cell. Human epidermis was chosen for the analysis, as it is generally considered more predictive of *in vivo* results.[28,29]

Results

Lipid nanoparticles

Physicochemical properties of pure lipid nanoparticles. Table 1 summarizes the physicochemical properties of pure lipid nanoparticles. LNPs formulated without PG had the largest hydrodynamic diameter (D_h) and exhibited considerable heterogeneity. At maximum colloidal concentration, aggregation was observed, likely due to the high lipid content and energy provided during sonication, which could hinder effective size reduction. It is well known that process parameters, such as the size reduction technique and the duration of sonication, are critical process parameters for lipid-based nanoparticles.[30,31] However, the present study focuses on the influence of colloidal concentration and PG content on the critical quality attributes, using a simple manufacturing method while maintaining all process parameters constant. Keeping these parameters constant allowed us to better highlight the role of lipid composition and colloidal concentration, and, most importantly, the impact of self-assembly on LNP performance, with distinct behavior observed for PG-containing LNPs, as described below.

Consistent with previous reports on the role of anionic lipids in colloidal stabilization,[32] replacing parts of the hydrogenated soy phosphatidylcholine (HSPC) with PG markedly improved the physicochemical properties of the LNPs. This effect, however, was not linear. Formulations containing a moderate amount of PG exhibited the smallest hydrodynamic diameters (129.7 ± 43.2–190.2 ± 25.8 nm) across all three colloidal concentrations tested: the formulation with the highest PG amount and colloidal concentration of 20 mg mL^{-1} displayed a comparably small D_h (182.9 ± 30.4 and 165.8 ± 27.9 nm, respectively).

PDI displayed a similar trend following PG incorporation in LNPs, reflecting improved particle size uniformity. The minimal PDI values (<0.1) were recorded for two formulations: 0.5 mg mL^{-1} PG at 10 mg mL^{-1} and 1 mg mL^{-1} PG at 20 mg mL^{-1}.

Zeta potential gives an indication of the potential stability of a colloidal system. A large negative or positive zeta potential repels the particles from each other and prevents them from flocculating. Interestingly, all formulations exhibited negative zeta potential, including those without PG. This may result from impurities in Phospholipon 90H or the inherent behavior of zwitterionic lipids, which can show negative zeta potential at pH 7.[33] Incorporation of PG further lowered zeta potentials to below −30 mV, indicating enhanced colloidal stability.[32] It is well established that nanoparticles exhibiting absolute zeta potential values above approximately 30 mV are generally considered stable over time, due to the presence of sufficient electrostatic repulsion.[34] In general, surface charge is primarily governed by ionic strength, pH, sample concentration, solvent viscosity, and chemical composition.[32,35,36] As expected, in the present study, lipid compositions differing in PG inclusion (presence or absence of PG) resulted in significant differences in zeta potential values. However, no significant variations were observed with respect to PG content (0.5 *vs.* 1 mg mL^{-1}), as shown in Table 1. This may suggest that electrostatic interactions at a molecular level on the nanoparticle surface are largely comparable among PG-containing formulations. The relatively small variations observed in zeta potential could also be attributed to the formation of similar surface morphologies across nanoparticles. Nevertheless, it should be noted that the behavior of nanoparticulate systems is inherently complex and influenced by multiple interacting parameters. Specifically, factors such as preparation protocol, lipid composition, lipid packing parameter, and colloidal concentration collectively affect curvature, structural organization, and the surface presentation of functional groups at the nanoparticle interface.[37] This is further supported by the impact of PG content and col-

Table 1 Physicochemical properties of pure lipid-based nanocarriers

PG (mg mL^{-1})	CollC (mg mL^{-1})	D_h (nm)	PDI	Zeta potential (mV)
0	10	363.5 ± 12.8	1.000	−26.6 ± 1.2
0	20	290.5 ± 168.1	1.000	−36.0 ± 0.8
0	20	287.0 ± 93.4	1	−23.8 ± 1.0
0	30	—[a]	—[a]	—[a]
0.5	10	167.5 ± 81.6	0.090 ± 0.030	−54.0 ± 1.4
0.5	20	168.2 ± 30.5	0.421 ± 0.040	−49.4 ± 1.5
0.5	20	190.2 ± 25.8	0.403 ± 0.169	−47.1 ± 1.2
0.5	20	129.7 ± 43.2	0.379 ± 0.278	−51.2 ± 0.7
0.5	30	156.9 ± 23.7	0.749 ± 0.356	−53.3 ± 6.5
1	10	272.4 ± 64.6	0.127 ± 0.070	−42.7 ± 1.2
1	20	182.9 ± 30.4	0.088 ± 0.010	−55.1 ± 1.8
1	20	165.8 ± 27.9	0.025 ± 0.010	−48.9 ± 0.7
1	30	309.3 ± 43.8	0.750 ± 0.121	−53.2 ± 1.5

[a] Not measured due to the formation of aggregates.

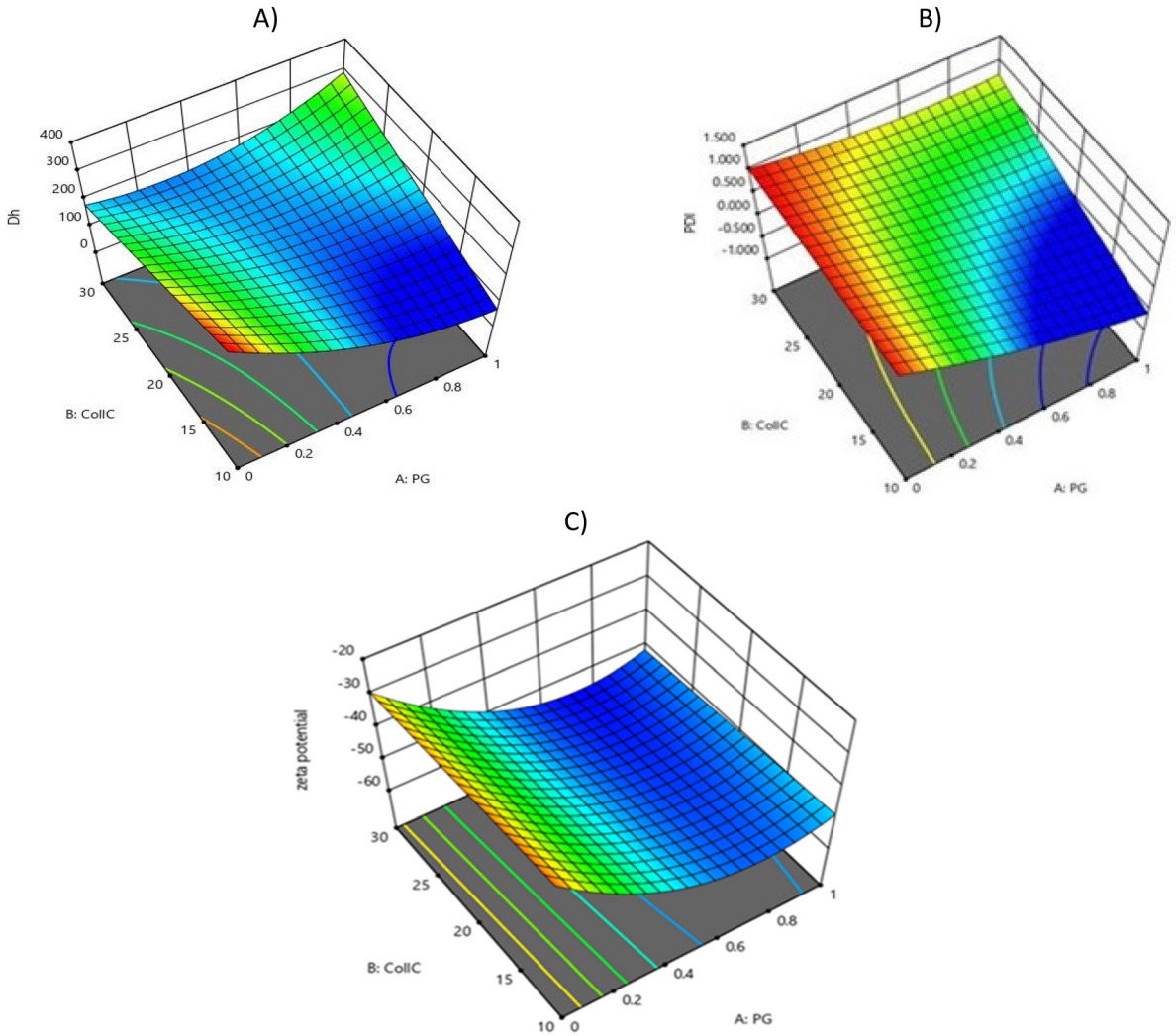

Fig. 1 3-D graphs that show how the two factors affect each response for the pure nanocarriers: (A) D_h, (B) PDI and (C) zeta potential, (Design Expert® – DX11). The blue areas correspond to the minimum values of the responses while as we approach the red areas the responses increase.

loidal concentration on surface curvature, which is reflected in changes in particle size, as discussed in more detail in the following paragraph.

The above observations were further supported by the 3D response-surface plots (Fig. 1). Regarding D_h, at low colloidal concentrations (≤15 mg mL^{-1}), increasing PG sharply reduced particle size, whereas moderate to high concentrations (≥15 mg mL^{-1}) displayed a particle size reduction with PG incorporation up to 0.5 mg mL^{-1} and a slight raise at higher PG levels. Formulations with medium PG levels maintained similar particle sizes across all concentrations, whereas PG-free systems and those containing the maximum amount of the anionic lipid exhibited a smaller D_h at a medium colloidal concentration (20 mg mL^{-1}).

Increasing the amount of anionic lipid resulted in a non-linear reduction of PDI, implying complex interactions within the system. Colloidal concentration also affected PDI in a non-linear way: at low PG levels, PDI values rose slightly with increasing concentration, whereas at higher PG content, an increase of concentration led to a more pronounced elevation of PDI, indicating aggregation and possible instability. Lastly, PG affected zeta potential independently of colloidal concentration; higher levels consistently produced more negative values, suggesting enhanced electrostatic stabilization.

Physicochemical properties of NIAC 1% lipid nanoparticles. Interestingly, the addition of niacinamide promoted the hydration of all thin films regardless of their lipid composition. As shown in Table 2, in the absence of PG and at the highest colloidal concentration, encapsulation efficiency could be measured; however, the physicochemical properties were not well-defined due to aggregation, as observed prior to the addition of niacinamide. Except for the systems with 30 mg mL^{-1} colloidal concentration and 0.5 or 1 mg mL^{-1} PG, niacinamide incorporation caused a slight increase in D_h. Regarding PDI, formulations without PG maintained a polydispersity index of 1 after niacinamide addition, indicating sub-

Table 2 Physicochemical properties and encapsulation efficiency of 1% NIAC lipid nanoparticles

PG (mg mL^{-1})	CollC (mg mL^{-1})	D_h (nm)	PDI	Zeta potential (mV)	EE%
0	10	379.3 ± 13.3	1.000	−32.2 ± 1.7	22.64
0	20	346.9 ± 20.4	1.000	−44.9 ± 1.6	16.15
0	20	358.0 ± 46.6	1.000	−40.1 ± 1.2	28.25
0	30	—[a]	—[a]	—[a]	20.38[a]
0.5	10	209.0 ± 32.1	0.199 ± 0.019	−65.8 ± 1.1	37.24
0.5	20	245.7 ± 10.7	0.145 ± 0.120	−67.9 ± 2.1	39.35
0.5	20	266.1 ± 18.7	0.135 ± 0.003	−61.2 ± 0.7	41.03
0.5	20	258.5 ± 16.4	0.162 ± 0.043	−62.3 ± 1.5	38.50
0.5	30	159.3 ± 33.3	0.315 ± 0.135	−64.8 ± 1.0	32.64
1	10	228.5 ± 24.1	0.298 ± 0.101	−77.4 ± 3.6	35.33
1	20	366.3 ± 12.6	0.097 ± 0.017	−70.2 ± 1.8	40.75
1	20	331.8 ± 23.5	0.139 ± 0.011	−72.6 ± 1.7	46.02
1	30	262.6 ± 17.4	0.160 ± 0.020	−75.3 ± 0.7	38.76

[a] Not measured due to the formation of aggregates.

stantial size heterogeneity, similar to the unloaded nanocarriers. In the remaining formulations, only minor changes in PDI were observed.

NIAC addition resulted in more negative zeta potential values for all LNPs, likely due to its partial deposition on the lipid bilayer surface. Having a pK_a equal to 3.3, niacinamide is expected to be fully deprotonated at pH 7, thereby contributing to the surface charge.

Formulations without PG displayed the lowest encapsulation efficiency values, not exceeding 28.25%. PG incorporation improved encapsulation up to a maximum of 46.02%, corresponding to the formulation containing 1 mg mL^{-1} PG at a colloidal concentration of 20 mg mL^{-1}. For the loaded NPs, the PG content plays a great role in the encapsulation efficiency of NIAC. Namely, the % EE of NIAC reached higher values as the concentration of PG increased (Table 2). NIAC is a small water-soluble molecule that is encapsulated into aqueous sub-compartments of the NPs and/or interacts *via* electrostatic and/or hydrogen bonds with head polar groups of PG.[38] This may cause increased membrane fluidity and alteration of phospholipid spacing. All the above may be indirect indications of changes in NPs' shape and surface morphology due to NIAC loading in comparison to pure NPs.

The 3D response-surface plots (Fig. 2) further illustrate the effects of PG and colloidal concentration on the LNPs' physicochemical characteristics and the NIAC encapsulation efficiency.

For hydrodynamic diameter (D_h), increasing PG up to moderate levels caused a significant decrease in particle size, whereas further addition of PG had the opposite effect. At low PG content, increasing colloidal concentration reduced D_h, whereas at medium and high PG contents, D_h initially increased and then decreased as concentration rose. In terms of formulation homogeneity, the incorporation of higher proportions of anionic lipid induces a non-linear decrease in the polydispersity index (PDI), suggesting improved size distribution uniformity. In contrast, increasing colloidal concentration produces an opposite effect, characterized by elevated PDI values. As shown in Fig. 2(c), increasing PG causes a non-linear reduction of zeta potential. Finally, increasing PG content enhanced encapsulation efficiency in a non-linear fashion, with moderate to high PG levels yielding the highest NIAC encapsulation.

Optimization. The goal of the study is to optimize the relationship between the variables and the responses, specifically to determine the appropriate levels of PG and colloidal concentration within their respective ranges that result in a formulation with minimum D_h, PDI, and zeta potential, while maximizing the encapsulation efficiency of niacinamide; all the above have a strong influence on the transdermal delivery.[39] The criteria for selecting the optimal formulations are presented in greater detail in Table 3. One of the design criteria is the zeta potential values that should be minimized. High zeta potential values in absolute terms are beneficial for the colloidal and long-term stability of the formulation. This parameter is also related to the skin permeation and retention ability of NPs.[35] Therefore, decreasing zeta potential values in this situation probably represents an optimization strategy to ameliorate a balance between improved skin interface and enough physicochemical stability, enabling a more effective drug delivery platform for NIAC.

Two of the five total optimal formulations with desirability 0.837 and 0.841, respectively, were designed: Optimal 1 – PG 0.8 mg mL^{-1} at a colloidal concentration of 10 mg mL^{-1} and Optimal 2 – PG 0.7 mg mL^{-1} at a colloidal concentration of 30 mg mL^{-1}. The LNPs were physicochemically characterized and the comparison of the actual and predicted values emerging from DoE for the physicochemical properties and encapsulation efficiency of NIAC are shown in Table 4.

***In vitro* skin permeation study of NIAC in lipid nanoparticles.** The two optimal formulations were chosen for further evaluation. A comparative *in vitro* epidermal permeation study was conducted where the non-optimal LNPs with the highest encapsulation efficiency (PG 1 mg mL^{-1}; CollC 20 mg mL^{-1}) and a 4.5% niacinamide solution served as references.

The herein developed niacinamide formulations were used *in vitro* without purification to have the same applied concen-

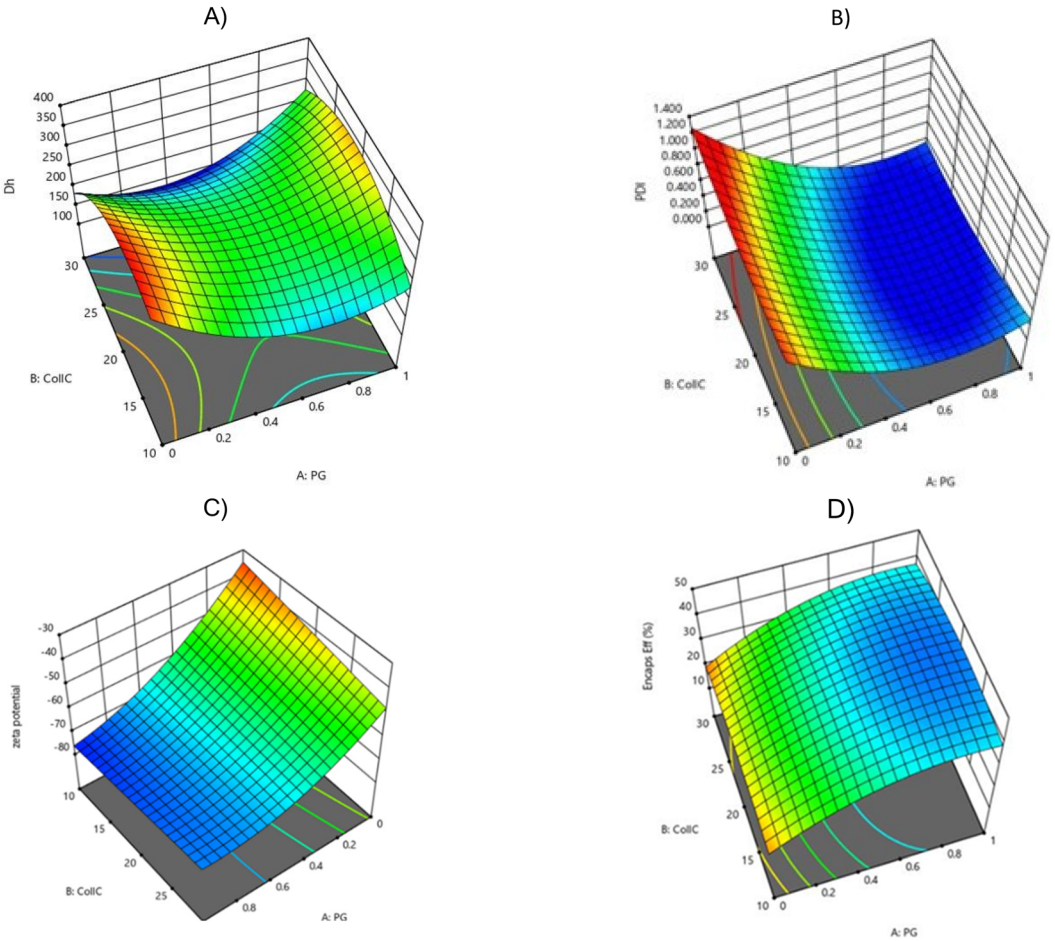

Fig. 2 3-D graphs that show how the two factors affect each response for the 1% NIAC lipid nanoparticles: (A) D_h, (B) PDI, (C) zeta potential and (D) EE (%), (Design Expert® – DX11). Blue colour indicates minimal values for D_h PDI and zeta potential and maximum values for EE.

Table 3 Criteria for designing the optimal formulations

Criteria	Goal	Significance
A (PG)	Within range	
B (CollC)	Within range	
Response 1 (D_h)	Minimize	++++
Response 2 (PDI)	Minimize	++++
Response 3 (zeta-potential)	Minimize	++++
Response 4 (EE)	Maximize	+++++

tration of niacinamide and nanoparticles in all cases, expecting for both encapsulated and unencapsulated NIAC to be affected by the presence of nanoparticles.[40]

Niacinamide skin permeation. The cumulative *in vitro* skin permeation of NIAC after 24 h is provided in Table 5. Results are expressed in terms of cumulative amount per unit area rather than steady-state flux (J, μg cm^{-2} h^{-1}) because the flux is calculated from the linear part of the curves, which usually occurs at longer times.[41]

Table 4 Comparison of the actual and predicted values for the physicochemical properties and encapsulation efficiency of the two optimal formulations

		Actual values	Predicted values	Difference %
Optimal 1	D_h (nm)	222.6 ± 31.3	205.0	−7.91
	PDI	0.163 ± 0.09	0.164	0.61
	Zeta potential (mV)	−70.3 ± 1.9	−72.30	2.85
	EE (%)	56.10	39.18	−30.16
Optimal 2	D_h (nm)	181.9 ± 0.4	179.4	−1.37
	PDI	0.150 ± 0.13	0.145	−3.33
	Zeta potential (mV)	−66.4 ± 0.9	−70.30	5.87
	EE (%)	44.90	37.57	−16.33

Table 5 Cumulative amount of NIAC Q (μg cm^{-2}) permeated per unit area ± SD

Time points	Optimal 1	Optimal 2	Non-optimal	NIAC 4.5% solution
3 h	4.56 ± 0.33	0.00	0.10 ± 0.29	0.22 ± 0.46
6 h	7.57 ± 0.78	2.77 ± 1.29	1.52 ± 0.55	0.12 ± 0.90
12 h	13.27 ± 1.76	13.21 ± 4.15	9.17 ± 1.63	3.77 ± 1.47
24 h	16.30 ± 1.87	16.02 ± 4.80	11.54 ± 2.04	5.57 ± 1.39

Statistical analysis demonstrated that for each formulation the data followed a normal distribution at all sampling time points. Furthermore, the two optimal formulations displayed a statistically significant difference at 3 and 6 hours that was not observed at later stages.

This difference is likely due to the high lipid concentration of Optimal 2, which potentially alters niacinamide diffusion and results in its slower release.[42]

The Optimal 1 formulation showed a statistically significant difference compared to both the non-optimal formulation and the NIAC 4.5% solution across all time points. On the contrary, the Optimal 2 formulation did not significantly differ from the non-optimal formulation and the macro formulation at 3 and 6 hours; statistically significant differences emerged at 12 and 24 hours. Finally, the non-optimal formulation also did not show a statistically significant difference from the NIAC solution at 3 and 6 hours; however, significant differences were observed at 12 and 24 hours.

The cumulative amount of niacinamide that permeated the skin from the two optimal formulations is higher than the corresponding amount that permeated from the non-optimal and considerably higher than the corresponding amount that permeated from the 4.5% NIAC solution. More specifically, the two optimal formulations achieved 192% more skin permeability relative to the macro formulation and 41% more compared with the non-optimal.

It is also observed that the optimal 1 formulation has zero lag time, whereas optimal 2 has a lag time equal to 0.81 h. Again, such a difference could be attributed to the different colloidal concentrations. The non-optimal nanoformulation has a lag time of 1.31 h, whereas the solution has the biggest lag time (2.49 h).

% Cumulative dose of niacinamide that permeated the skin. As seen on Table 6, large differences were observed across the different formulations concerning the % cumulative dose of niacinamide that permeated the skin. The optimal formulations deliver about 1.5% of the dose they contain; the non-optimal delivers 1.1%, while the solution appears to deliver about 0.1%. All the percentage data follow a normal distribution at every sampling time point. The statistical differences are according to the ones resulting from the comparison of the cumulative amount of NIAC that permeated the skin from each formulation.

Fig. 3 presents cumulative NIAC permeation per unit area (amount and percentage dose) for the two optimal LNPs relative to the remaining formulations and highlights differences in the corresponding lag times.

Niacinamide skin retention. The NIAC retention in human stratum corneum is provided in Fig. 4 and Table 7, while the NIAC retention percentage is also given in Fig. 4. All the skin retention data follow a normal distribution at 24 hours. As proven in previous studies,[43,44] lipid nanoparticles may enhance the skin retention of both hydrophilic and lipophilic molecules. Indeed, the two optimal LNPs demonstrated increased retention of niacinamide in the human stratum corneum with no statistically significant difference observed between them, in contrast to the other formulation comparisons. The non-optimal lipid nanocarrier also showed a notable skin retention of the compound, whereas the solution had the least skin retention by far. The optimal formulations exhibited 21.68% and 13.70% more skin retention, respectively, compared to the non-optimal. The NIAC amount deposited in the skin from the optimal LNPs was approximately 11–12 times greater than the solution.

In vitro studies are generally considered a preliminary step towards *in vivo* evaluation and clinical translation. However, the herein developed lipid nanoparticles displayed a significant amelioration of permeation and retention of NIAC in the skin compared with the reference solution, despite the lower concentration of the molecule. Noteworthy, the experiments were conducted using human epidermis, which, as mentioned above, is considered more predictive of *in vivo* outcomes. Therefore, the improved delivery performance suggests that the optimized LNPs could represent a promising drug delivery platform with potential therapeutic relevance. Lastly, as reported by Lee *et al.*,[3] who also formulated lipid-based nanocarriers, similar improvements of NIAC permeation and deposition in the skin were linked with enhanced whitening effects, hence supporting the plausibility of therapeutic potential.

Polymeric nanoparticles

Physicochemical properties of pure polymeric nanoparticles. For the pure polymeric formulations, D_h exhibited a nonlinear behaviour with concentration (Table 8). At 10 mg mL^{-1}, rela-

Table 6 Cumulative (%) dose of NIAC that permeated the skin

Time points	Optimal 1	Optimal 2	Non-optimal	NIAC 4.5% solution
3 h	0.4265 ± 0.0637	0.0010 ± 0.021	0.0016 ± 0.017	0.0001 ± 0.0001
6 h	0.7092 ± 0.0963	0.2597 ± 0.1057	0.1449 ± 0.0781	0.0071 ± 0.0045
12 h	1.2457 ± 0.2749	1.2375 ± 0.2926	0.8789 ± 0.1564	0.0801 ± 0.0217
24 h	1.5306 ± 0.2243	1.5011 ± 0.3392	1.1071 ± 0.1617	0.1181 ± 0.0224

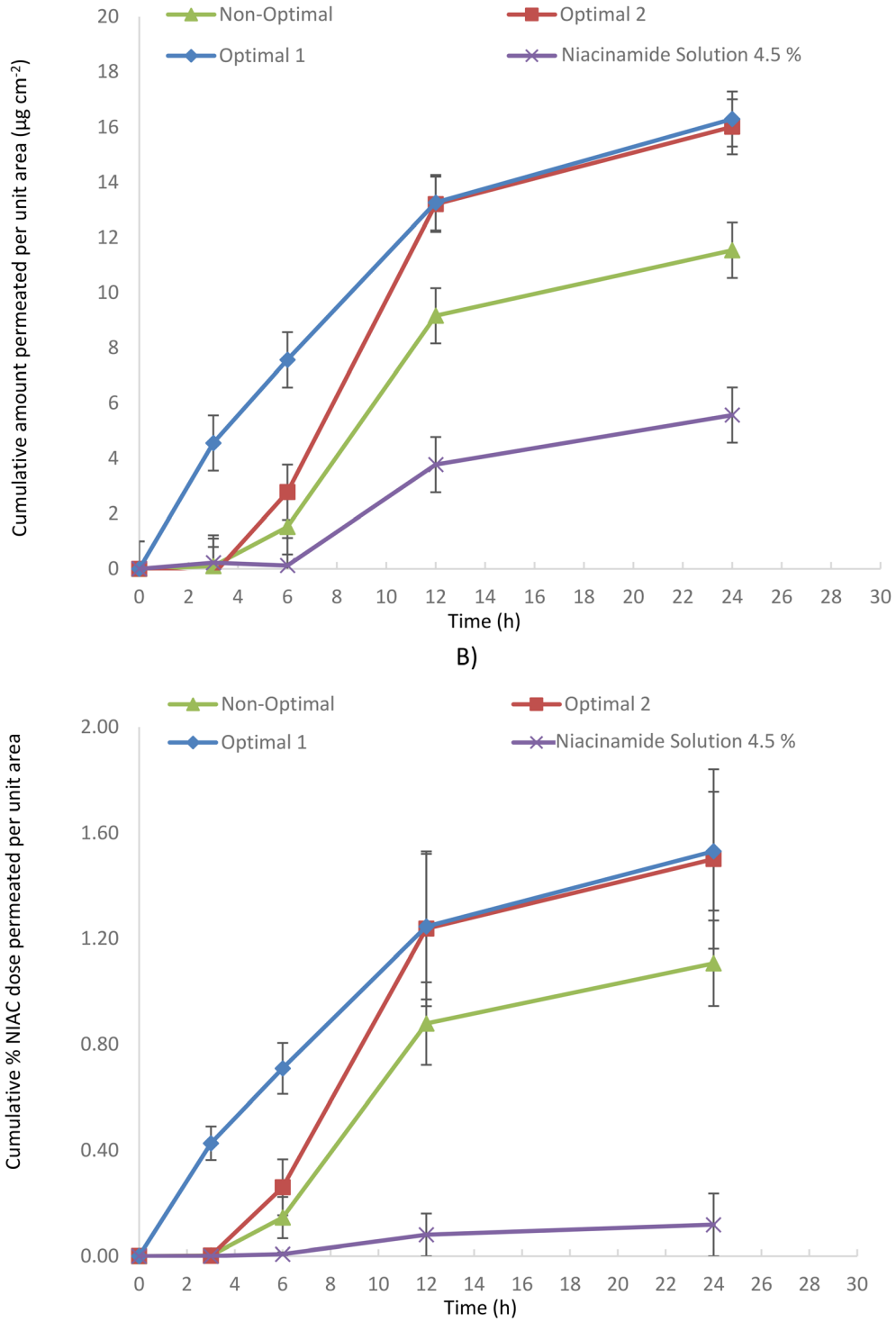

Fig. 3 Cumulative amount of NIAC (μg cm^{-2}) (A) and Cumulative %NIAC dose (B) permeated per unit area.

tively small particles were observed (147.5 ± 4.8 nm), which increased markedly at 20 mg mL^{-1} (455.4 ± 23.9 nm) and decreased again at 30 mg mL^{-1} (295.0 ± 25.8 nm). The PDI values were moderately high across all concentrations (0.581–0.651), suggesting broad size distributions and a relatively polydisperse colloidal population. Notably, polymer concentration did not seem to have a significant impact on the PDI of pure nanocarriers, suggesting that the observed heterogeneity is intrinsic to the system under these formulation parameters. This behavior may be attributed to the employment of the single polymer Kolliphor® P407, which, in combination with the relatively mild preparation conditions, may provide

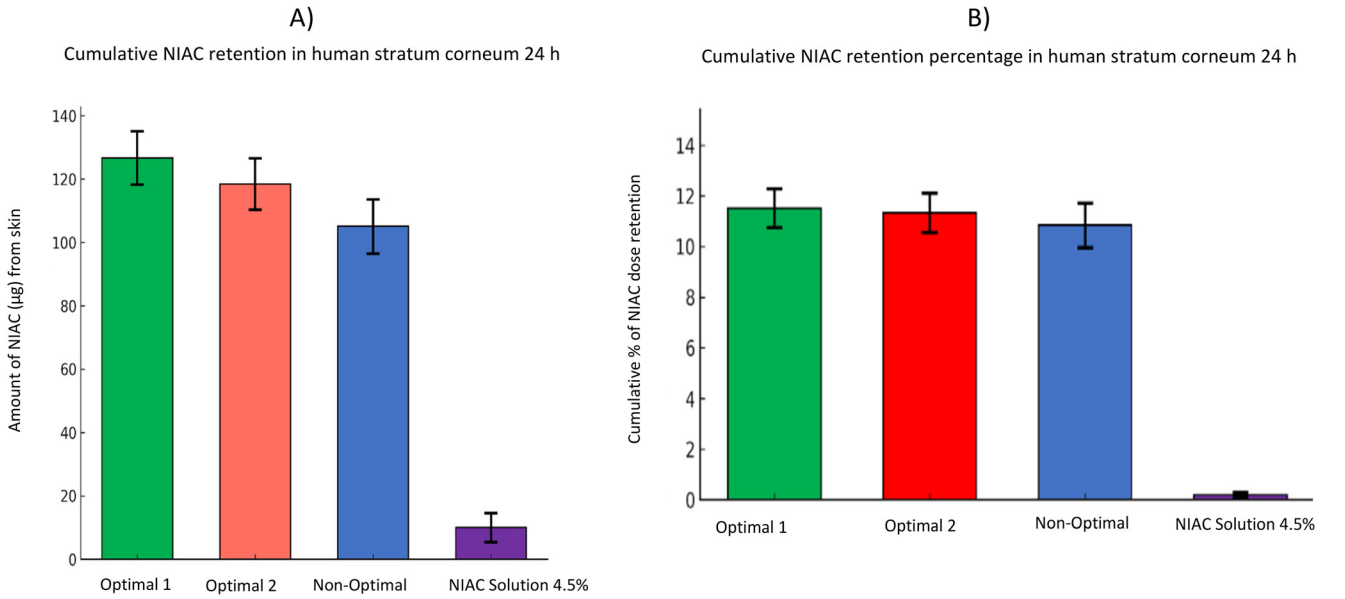

Fig. 4 Cumulative NIAC (A) and % NIAC (B) retention in human stratum corneum at 24 h.

Table 7 Cumulative NIAC retention in human stratum corneum for lipid based and reference formulations and cumulative NIAC retention percentage in human stratum corneum (mean ± SD, n = 6)

	Optimal 1	Optimal 2	Non-optimal	NIAC solution 4.5%
NIAC skin retention (µg)	126.70 ± 8.44	118.45 ± 8.12	105.05 ± 8.51	10.01 ± 4.53
% NIAC skin retention	11.90 ± 1.00	11.11 ± 0.73	10.09 ± 0.58	0.21 ± 0.09

Table 8 Physicochemical properties of pure polymer-based nanocarriers

Concentration (mg mL^{-1})	D_h (nm)	PDI	Zeta potential (mV)
10	147.5 ± 4.8	0.614	−5.0 ± 1.0
20	455.4 ± 23.9	0.651	−15.3 ± 2.3
30	295.0 ± 25.8	0.581	−11.4 ± 3.2

Table 9 Physicochemical properties of NIAC polymeric nanoparticles

Concentration (mg mL^{-1})	D_h (nm)	PDI	Zeta potential (mV)	EE(%)
10	188.9 ± 10.8	0.456	−8.3 ± 2.4	5.58 ± 1.43
20	671.6 ± 23.6	0.836	−23.8 ± 3.9	9.00 ± 0.40
30	287.6 ± 21.8	0.557	−33.0 ± 2.8	7.10 ± 1.60

limited colloidal stabilization in comparison to more structurally complex polymeric systems. All formulations exhibited slight negative surface charges (−5.01 mV to −15.33 mV), indicative of limited electrostatic stabilization.

Physicochemical properties of NIAC polymeric nanoparticles. The presence of niacinamide, as shown in Table 9, markedly influenced the physicochemical features of the vector. Overall, the 10 mg mL^{-1} niacinamide-containing formulation displayed the most favorable colloidal features, characterized by a relatively small D_h and the lowest PDI value within the tested formulations. At the minimum polymer concentration, niacinamide caused a slight increase in D_h (189.9 ± 10.8 nm) and a clear reduction in PDI (0.456), suggesting different molecular interactions leading to different self-assembly. This effect is likely associated to interactions between niacinamide—a polar, hydrophilic molecule—and the micellar corona of Kolliphor® P407, which modestly enlarges the micelles, while stabilizing the structure.

In contrast, at 20 mg mL^{-1} the hydrodynamic diameter increased substantially to 671.6 ± 23.6 nm, accompanied by a pronounced rise in polydispersity (PDI = 0.836), consistent with the formation of larger, more heterogeneous aggregates. We assume that this transition reflects entry into a concentration regime near a critical self-assembly threshold, where intermicellar association and multicore structures are favored. These interactions enlarge the assemblies and broaden the size distribution, as reflected by the higher PDI relative to the mg mL^{-1} formulation.

Finally at 30 mg mL^{-1}, the size and polydispersity are similar to those of the pure formulation (D_h = 287.6 ± 21.8 nm; PDI = 0.557), indicating that niacinamide at this concentration level does not have a great effect on the configuration.

Interestingly, the presence of niacinamide resulted in pronounced changes in PDI values, and unlike the pure nanocarriers, a marked association with polymer concentration was detected. Such findings suggest that the interaction between the hydrophilic molecule and the Kolliphor® P407 micelles may influence their self-assembly behavior, plausibly leading to the formation of different micellar structures in a non-linear, polymer concentration-dependent manner.

Considering the zeta potential after the addition of NIAC, it became progressively more negative, reaching −33.0 ± 2.8 mV at 30 mg mL^{-1}, probably due to the full deprotonation of NIAC at pH 7.0 as mentioned before. The shift of zeta potential to lower values by increasing the total concentration also supports the presence of NIAC on the surface of the structure. Moreover, a zeta potential with an absolute value greater than 30 mV would typically suggest improved colloidal stability due to electrostatic repulsion; however, the concurrent increase in D_h and PDI at 20 mg mL^{-1} implies that additional mechanisms may overcome electrostatic stabilization and promote aggregation at intermediate concentrations.

Compared to alternative nanocarriers, polymeric micelles generally demonstrate modest encapsulation efficiency values. Their intrinsic architecture – consisting of a relatively small hydrophobic core surrounded by a hydrophilic corona – restricts the available volumetric capacity for drug sequestration, thereby limiting the payload capacity.[45] Moreover, the thermodynamic driving force for micelle formation is primarily governed by hydrophobic interactions. Consequently, drugs that are not strongly hydrophobic are poorly partitioned into the core and rapidly dissociate upon dilution in physiological media.[45] The incorporation of hydrophilic drugs is therefore thermodynamically unfavorable, resulting in markedly lower drug loading capacities and encapsulation efficiencies compared to hydrophobic drugs.[46] This limitation is often identified as a significant obstacle for amphiphilic polymeric micelles, which are known to have a low drug loading capacity when used with water-soluble agents.[45] The encapsulation efficiency (EE%) values obtained for all three formulations reveal a system capable of entrapping a hydrophilic compound within a micellar structure, although the overall efficiencies remain modest. This outcome aligns with literature reports describing similar behaviors for hydrophilic molecules such as niacinamide, which tend to partition preferentially into the aqueous phase rather than the hydrophobic micellar core. At 10 mg mL^{-1}, the formulation exhibited an EE% of 5.58 indicating that micellar structures formed efficiently and were capable of incorporating niacinamide even at relatively low polymer concentrations. Although the encapsulation efficiency at this concentration was limited, it highlights the ability of the system to achieve drug loading despite the molecule's hydrophilic nature and low affinity for hydrophobic environments. Increasing the polymer concentration to 20 mg mL^{-1} led to the highest EE% (9.0%). This enhancement can be attributed to the higher availability of hydrophilic polymer chains and the formation of a larger number of micellar aggregates, which provide more sites for drug association. At the highest concentration tested, 30 mg mL^{-1}, the EE% slightly decreased. This result could indicate that excessive polymer content alters the micellar organization or increases the viscosity of the dispersion medium, hindering drug diffusion into the micellar core. Overall, the observed trends suggest that polymer concentration plays a key role in modulating encapsulation capacity, and fine-tuning this parameter could positively influence drug loading efficiency.

***In vitro* skin permeation study of NIAC in polymeric nanoparticles.** The cumulative amount of NIAC permeated per unit area for the three polymeric nanoparticles is presented in Table 10 and Fig. 5. The 10 mg mL^{-1} formulation exhibits a lag time of around 3 hours, followed by a gradual and sustained permeation process that achieves a cumulative value of 11.8 μg cm^{-2} within 24 hours. This behaviour is consistent with the small micelle size and low polydispersity index observed, which are indicative of a stable micellar system tending toward homogeneity. The initial delay in permeation observed could be attributed to the high structural stability, which limits the release of the encapsulated drug.[47] Despite the relatively modest encapsulation efficiency, not all of the free niacinamide is immediately available for diffusion. In fact, it takes time for the system to reach dynamic equilibrium between the free fraction and the fraction associated with the micelles. Once equilibrium is reached, the niacinamide becomes progressively available, resulting in constant, controlled diffusion over time. This is indicative of an efficient, thermodynamically balanced release process. By contrast, the 20 mg mL^{-1} formulation showed immediate release (no lag time) and the highest cumulative permeation (~11.9 μg cm^{-2}). The free-drug concentration is approximately twice that of the 10 mg mL^{-1} formulation, providing a stronger thermodynamic drive for diffusion.

This aligns with the diffusive flow equation:

$$J = (D_m C_{s,m}/L)(c_v/c_{s,v}),$$

where D_m is the diffusion coefficient in the membrane, $C_{s,m}$ the drug solubility in the membrane, c_v the drug concentration in the vehicle, $c_{s,v}$ its solubility in the vehicle, and L the membrane path length.[48] As $c_v/c_{s,v}$ increases, flux rises, steepening the concentration gradient and accelerating permeation. In contrast, the 30 mg mL^{-1} formulation exhibited a prolonged lag (~6 h), lower cumulative permeation (~5.9 μg cm^{-2}; ~half of 20 mg mL^{-1}), and overall slower kinetics. Increasing micelle/polymer content promotes transient polymer–micelle networking that elevates zero-shear viscosity, suppresses mole-

Table 10 Cumulative amount of NIAC (μg cm^{-2}) permeated per unit area ± SD

Time points	10 mg mL^{-1}	20 mg mL^{-1}	30 mg mL^{-1}
3 h	0.00 ± 0.33	2.40 ± 0.35	0.00
6 h	3.51 ± 0.93	4.54 ± 0.29	0.00 ± 0.46
12 h	8.31 ± 0.93	8.36 ± 1.96	2.63 ± 0.37
24 h	11.77 ± 0.79	11.92 ± 1.82	5.95 ± 0.50

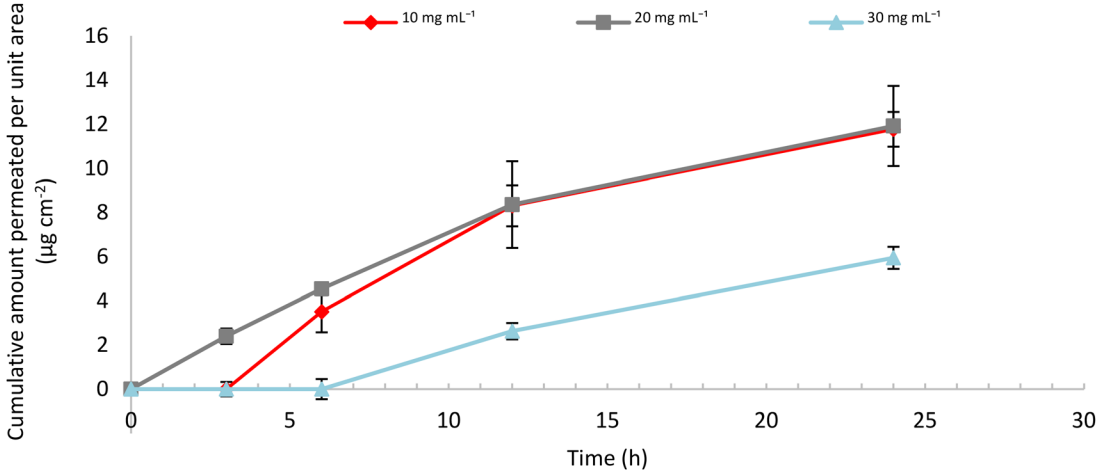

Fig. 5 Cumulative amount of NIAC (μg cm^{-2}) permeated per unit area.

cular mobility, and lowers ionic conductivity—hallmarks of fewer freely mobile species.[49] Indeed, the higher viscosity and micellar density at 30 mg mL^{-1} likely hinders niacinamide diffusion and prolongs lag time. Stronger drug–polymer interactions at high concentration may further slow drug release from micelles, lowering thermodynamic activity and thereby reducing membrane permeation efficiency.

Niacinamide skin retention. The NIAC retention in human stratum corneum is provided in Fig. 6 and Table 11, while the NIAC retention percentage is also given in Fig. 6. The physical–chemical balance of the micellar system has a decisive influence on its ability to interact with the skin surface and, consequently, on the skin retention of the encapsulated compound. The 10 mg mL^{-1} formulation resulted in the highest cumulative retention of niacinamide in the human stratum corneum after 24 hours, both in terms of absolute quantity (7.21 ± 0.67 μg) and as a percentage of the applied dose (6.80 ± 0.63%). In contrast, the 20 mg mL^{-1} and 30 mg mL^{-1} formulations showed lower values (5.28 ± 0.89 μg–7.47 ± 2.34 μg, respectively), equal to 2.52 ± 0.45%–2.39 ± 0.75% of the applied dose. These results indicate that the weakly negative zeta potential observed for the 10 mg mL^{-1} formulation (−8.3 ± 2.4 mV), together with its optimal size (189.9 ± 10.8 nm) and colloidal homogeneity (PDI: 0.456), plays a decisive role in promoting more effective interaction with the lipid matrix of the stratum corneum and, consequently, superior skin retention of the active ingredient. This profile represents an optimal condition, in which the repulsive forces towards the epidermal surface are attenuated, while maintaining a sufficient charge to ensure colloidal stability. Conversely, the increase in zeta potential negativity in the 20 mg mL^{-1} and 30 mg mL^{-1} formulations (−23.8 ± 3.9 mV and −33.0 ± 2.8 mV, respectively) intensifies electrostatic repulsion from the skin surface and combined with larger size and greater polydispersity, reduces skin retention.

Regarding the polymeric nanoparticles, results suggest a comparable delivery performance to the reference solution with improved permeation demonstrated in most cases, although skin retention was found to be lower. As discussed above, incorporation of hydrophilic molecules into polymeric micelles is thermodynamically unfavorable and typically yields modest encapsulation efficiency values, as observed for niacinamide in the present study. Additionally, the significantly lower NIAC concentration employed in the polymeric nanocarriers, in comparison to both the reference solution and the lipid nanoparticles, should be taken into consideration when interpreting these findings. Despite the restrictions, the permeation profiles indicate that polymeric nanoparticles may facilitate niacinamide transport across the skin and should be further investigated.

Overall, both lipid- and polymer-based nanocarriers led to interesting findings, and their clinical value should be elucidated more extensively through *in vivo* studies.

Materials and methods

Materials

For the preparation of LNPs LIPOID PG 16 : 0/16 : 0 (1,2-dipalmitoyl-*sn-glycero*-3-phosphoglycerol sodium salt, DPPG-Na) and PHOSPHOLIPON® 90 H (Hydrogenated Phosphatidylcholine from Soybean) were purchased from Lipoid GmbH (Ludwigshafen am Rhein, Germany). Kolliphor® P407 Geismar (poloxamer 407) was obtained from BASF Corporation (8404 River Road, Geismar, LA 70734, USA).

Chloroform and methanol of HPLC-Grade served as organic solvents for the lipids. Niacinamide was bought from Fagron Hellas (Trikala, Greece). Glycerin and Propylene Glycol were bought from Chemco®-Syndesmos (Athens, Greece).

For the high-performance liquid chromatography (HPLC) analysis and niacinamide extraction, acetonitrile, water and methanol of HPLC-Grade were used. For the IVPT, HPLC-grade water, sodium phosphate monobasic dihydrate and sodium hydroxide were used. All materials were of pharmaceutical grade.

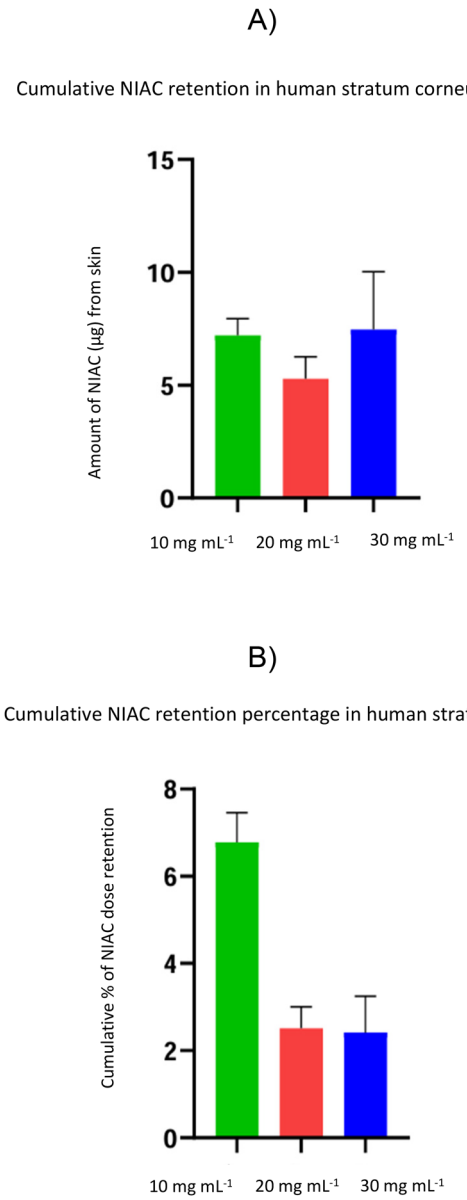

Fig. 6 Cumulative NIAC (A) and % NIAC (B) retention in human stratum corneum at 24 h.

Table 11 Cumulative NIAC retention in human stratum corneum for NIAC polymeric nanoparticles and cumulative NIAC retention percentage in human stratum corneum (mean ± SD, n = 6)

	10 mg mL^{-1}	20 mg mL^{-1}	30 mg mL^{-1}
NIAC skin retention (µg)	7.21 ± 0.67	5.28 ± 0.89	7.47 ± 2.34
% NIAC skin retention	6.80 ± 0.63	2.52 ± 0.45	2.39 ± 0.75

Design of experiments

The analysis of the Experimental Design results was performed using the Design-Expert® Software Version 11 (Statease, Minneapolis, USA).

Table 12 Independent variables and their levels used in the experimental design

Factor	Variable	Type	Units	Low (−1)	Center (0)	High (1)
A	PG	Numeric	mg mL^{-1}	0.0	0.5	1
B	CollC	Numeric	mg mL^{-1}	10.00	20.00	30.00

Table 13 Experimental design matrix showing coded and actual levels of independent variables – with 4 repetitions (2 at the central point and 1 at each extreme value of PG)

Run	Coded A	Coded B	PG (mg mL^{-1})	CollC (mg mL^{-1})
12	−1	−1	0.0	10.00
2	−1	0	0.0	20.00
10	−1	0	0.0	20.00
3	−1	1	0.0	30.00
4	0	−1	0.5	10.00
7	0	0	0.5	20.00
9	0	0	0.5	20.00
11	0	0	0.5	20.00
13	0	1	0.5	30.00
1	1	−1	1.0	10.00
5	1	0	1.0	20.00
8	1	0	1.0	20.00
6	1	1	1.0	30.00

A factorial experimental design with two factors at three levels was applied. The factors and their limits, as well as the DoE matrix are shown at Tables 12 and 13 respectively.

Preparation of lipid nanoparticles

Stock solutions of the two lipids were prepared. For HSPC, the concentration of the solution was 20 mg mL^{-1}, and it was achieved by dissolving the lipid in the appropriate amount of chloroform, whereas for PG, the concentration of the solution was 1 mg mL^{-1} and the solvents used were chloroform and methanol at a 9 : 1 volume ratio. As mentioned before, the lipid nanoparticles were prepared with the thin film hydration method. Each time appropriate amount of stock solutions was added in a round flask and then the organic solvents were evaporated using a rotatory evaporator, to leave behind a thin, dry lipid film on the walls of the flask. The LNPs are finally obtained by hydrating the thin film with water of HPLC-Grade for the pure nanocarriers and with NIAC aqueous solution 1% w/v for the loaded systems. The temperature during the hydration phase was 60 °C and it was chosen based on the transition temperatures (T_m) of the lipids (~55 °C for HSPC and ~41 °C for PG). For further size reduction of the LNPs, bath sonication was performed using an ultrasonic bath (Elmasonic S, Elma, Germany) for 15 minutes at 60 °C under continuous operation to keep bilayers fluid during the procedure.[50,51] The temperature was controlled throughout the procedure with the built-in heating system of the ultrasonic bath. The sonication conditions were selected based on prior research utilizing HSPC liposomal formulations.[52]

Preparation of polymer nanoparticles

Polymeric micelles were prepared using the bath sonication method. The water bath temperature was maintained at 45 °C throughout the process using a digital temperature controller. Three blank micellar formulations with polymer concentrations of 10 mg mL^{-1}, 20 mg mL^{-1}, and 30 mg mL^{-1} were initially prepared to assess the effect of polymer concentration on the physicochemical properties of the micelles, while all process parameters (temperature, sonication time, and cycle conditions) were kept constant. Subsequently, three niacinamide-loaded formulations were prepared at the same concentrations with a polymer-to-drug ratio of 9 : 1. Each preparation cycle consisted of three sonication steps of 10 minutes, each separated by 10 minutes of break. These breaks were introduced to allow annealing, thereby facilitating the stabilization of the system into a new metastable state and promoting the self-assembly of the polymer into micellar structures.

Physicochemical characterization

The size (hydrodynamic diameter, D_h), size distribution (polydispersity index, PDI) and zeta potential of the herein developed nanoparticles were assessed by dynamic and electrophoretic light scattering (DLS and ELS) techniques. Particle size and polydispersity index were measured on a HORIBA nanoPartica SZ-100 (V2 series) using DLS at a 90° scattering geometry with a 532 nm laser, under temperature control (25 °C). Samples were diluted in HPLC grade water to minimize multiple scattering; the refractive index and viscosity of the medium were entered into the software prior to analysis. For each sample, 3 runs were collected and the *Z*-average hydrodynamic diameter and PDI (cumulants analysis) were reported. Zeta potential was determined by laser Doppler electrophoresis in disposable zeta cells with built-in electrodes. A background electrolyte was used to control ionic strength; pH was adjusted as required. Electrophoretic mobility was converted to zeta potential using the Smoluchowski model and results are reported as mean ± SD from 3 replicates.

Encapsulation efficiency

Encapsulation efficiency (% EE) of niacinamide was measured by using a dialysis method. Firstly, 500 μL of NIAC-loaded lipid or polymeric nanoparticle dispersion was added into cellulose dialysis tubing with a molecular weight cut-off (MWCO) of 12 000 Da (Sigma-Aldrich, Rancho Dominguez, CA, USA). The dialysis sack was then sunk into a beaker containing 25 mL of HPLC-grade H_2O and stirred for 30 minutes at 700 rpm at room temperature (25 °C). Afterwards, a sample of the solution was withdrawn and the amount of non-encapsulated NIAC in the external dialysis medium was quantified by HPLC, as described in detail in the corresponding section.

The encapsulation efficiency (EE%) of niacinamide within the nanoparticles was finally calculated using the following equation:

$$EE\% = \text{encapsulated niacinamide/total niacinamide} \times 100.$$

Reference formulation preparation

A niacinamide solution 4.5% w/v was prepared for HPLC analysis, as a reference of the permeation study. The reference solution was formulated by dissolving the appropriate amount of NIAC to a mixture of HPLC water, Glycerin and Propylene Glycol at a volume ratio of 67 : 5 : 27.

The reference formulation derives from previous studies in our lab, where the 3 solvents, water, glycerin, and propylene glycol, were chosen based on literature,[53] and the utilization of the Formulating for Efficacy™ (JW Solutions) software. The selected solvent ratio was a result of an optimization study with the use of Design of Experiments, targeting maximal thermodynamic activity at 95% of the saturation concentration in the formulation, aiming to achieve maximal transdermal permeation.

HPLC analysis

UV/Vis analysis using a Shimadzu PharmaSpec UV-1700 UV/Vis spectrophotometer (Shimadzu Europa GmbH) was performed solely for the determination of the maximum absorption wavelength (λ_{max}) of niacinamide, which was found to be 254 nm.

All quantitative analyses, including encapsulation efficiency, skin permeation, and skin retention, were performed using HPLC with UV detection, based on the method described by Thomas *et al.*[54] The HPLC system consisted of a high-pressure pump (P1000, Spectra Physics, USA), an automatic sampler (AS1000, Spectra Physics, USA), a system control unit (Spectra System SN 4000, Thermo Separation Products, USA), and a UV-Vis detector (Spectra System 2000, Thermo Separation Products, USA). The Intersil ODS-2 column (250 × 4.6 mm, 5 μm) was selected as the stationary phase. Chromatographic analysis was performed using a mobile phase of MeOH and 0.02 M phosphate buffer (40 : 60, pH 5.5) at a flow rate of 1.0 mL min^{-1}. UV detection was set at λ = 254 nm with an injection volume of 50 μL and NIAC exhibited a retention time of 3.45 min under these conditions.

Limit of Detection (LOD) and Limit of Quantification (LOQ) were calculated based on signal-to-noise ratio (S/N). Noise multiplied by 3.3 for LOD and 10 for LOQ. LOD and LOQ were estimated to be 0.2463 μg mL^{-1} and 0.7463 μg mL^{-1}, respectively. According to the above values, calculated from calibration curve data, all the HPLC analysis results are above the limit of detection and limit of quantification and thus confirm the validity of the analytical method. Linearity was assessed by ANOVA analysis using GraphPad Instat 3.05 (USA) to determine the correlation coefficient (R) and P value. The standard calibration curve was linear in the range of 1–10 μg mL^{-1} (R > 0.999 and P < 0.0001). For samples with higher concentration levels, a second calibration curve in the range of 1–50 μg mL^{-1} was also utilized, where the LOD and LOQ were calculated to be 0.9082 μg mL^{-1} and 2.7520 μg mL^{-1}, respectively.

In vitro permeation study

Cumulative skin permeation was assessed with vertical Franz diffusion cells of total volume 6.275 mL and total area avail-

able for diffusion 0.636 cm^2, mounted with human stratum corneum. Human epidermis was excised according to heat separation protocol and stored in refrigerator at −15 ± 2 °C. The amount of each formulation (the three LNPs with 1 NIAC %, the three NIAC polymeric nanoparticles and the reference solution 4.5%) placed in the donor compartment, to ensure uniformity, was approximately 100 mg. The experiment was performed in a water bath with a stable temperature at 32 °C ± 1, under magnetic stirring at 600 rpm. Franz cells with human stratum corneum were left for 12 h with the receptor solution in the water bath before the initiation of the experiment, for the stratum corneum to hydrate. For each formulation, 6 cells were used. Receptor fluid was PBS solution, with pH 7.4 and the selection was based on a previous study from Lee.[3] The total volume of the receptor fluid was sampled and replaced with fresh receptor fluid, at 3, 6, 12 and 24 h. Samples were analysed undiluted.

Mass balance

To ensure the validity of the permeation results and depict more accurately niacinamide's distribution in the tissue, mass balance calculations were performed. NIAC from the donor compartment was extracted, to calculate the amount that did not leave the formulation to penetrate and permeate the human stratum corneum. The donor compartment was washed 5 times with extraction solution (PBS solution pH 7.4).[3] The diluents were accumulated in volumetric flasks and diluted to 100 mL, with extraction solution. Samples were then diluted accordingly and quantified by using HPLC-UV method. Niacinamide retained in the human stratum corneum was quantified after extraction from the tissue in test. Extraction solution (1 mL) was placed with the entire *ex vivo* tissue from each Franz cell in a 1.5 mL Eppendorf tube and kept refrigerated overnight, followed by centrifugation at 5000 rpm for 5 min at 25 °C using a HERMLE Type Z 32 HK centrifuge (Labortechnik GmbH, Germany). The supernatant was diluted accordingly to be analyzed with HPLC.[40]

Statistical analysis

For the analysis of the obtained raw data, Excel® (Microsoft Office 365) was used. Statistical analysis (normality test, ANOVA, paired *t*-test and Tukey's multiple comparisons test) was performed with GraphPad Prism 10.5.0. (GraphPad Software®). Statistical differences were considered significant at $p < 0.05$. Results are expressed as mean values ± SD.

Conclusions

1% NIAC was successfully formulated in PG nanoparticles, prepared by a simple thin-film hydration method. The effects of PG and colloidal concentration on physicochemical properties, as well as on the encapsulation efficiency of NIAC, were determined and optimized with the use of Design of Experiments (DOE). Results showed that incorporation of PG favorably influences both responses. *In vitro* skin permeation testing (IVPT) using Franz diffusion cells demonstrated substantially improved skin permeation and retention of NIAC from the two optimal formulations compared to both a non-optimal nanocarrier and a NIAC solution with a significantly higher concentration (4.5%). Additionally, three NIAC polymeric micellar systems were prepared using bath sonication and evaluated *in vitro.* Overall, the results showed that increasing the total polymeric and compound concentration does not lead to a proportional increase in transdermal permeation; rather, the physicochemical and colloidal properties of the system have a decisive influence on diffusion kinetics. The 10 mg mL^{-1} formulation appears to be the most promising micellar system for transdermal delivery of niacinamide, balancing between colloidal stability, structural homogeneity, and release capacity, while also providing controlled and steady permeation. This study explores the potential of PG nanoparticles and highlights the importance of nanocarrier optimization for enhancing delivery through skin. It could be a valuable roadmap for formulation scientists to refine, verify, and advance LNP formulations, while it also demonstrates the potential of polymeric nanoparticles for improved transdermal delivery, even of highly hydrophilic substances.

Author contributions

Dimitra Bompou: methodology, validation, investigation, formal analysis, visualization, writing – original draft. Emanuela Di Biase: methodology, validation, investigation, formal analysis, visualization, writing – original draft. Alexandra Sarika: methodology, validation, investigation. Efstathia Triantafyllopoulou: methodology, validation, investigation. Natassa Pippa: conceptualization, resources, supervision, writing – review & editing. Dimitrios M. Rekkas: supervision, writing – review & editing. Paraskevas Dallas: conceptualization, resources, supervision, writing – review & editing.

Conflicts of interest

The authors declare no conflicts of interest.

Data availability

The data supporting the findings of this study are available within the article.

Acknowledgements

The authors wish to thank Professor Vassilios Roussis and his colleagues for the provision of facilities for the size, and zeta-potential measurements.

References

1 C. Marques, F. Hadjab, A. Porcello, K. Lourenço, C. Scaletta, P. Abdel-Sayed, N. Hirt-Burri, L. A. Applegate and A. Laurent, *Antioxidants*, 2024, **13**, 425.
2 W. Gehring, *J. Cosmet. Dermatol.*, 2004, **3**, 88–93.
3 M. H. Lee, K. K. Lee, M. H. Park, S. S. Hyun, S. Y. Kahn, K. S. Joo, H. C. Kang and W. T. Kwon, *J. Drug Delivery Sci. Technol.*, 2016, **31**, 147–152.
4 J. Wohlrab and D. Kreft, *Skin Pharmacol. Physiol.*, 2014, **27**, 311–315.
5 D. Mohammed, J. M. Crowther, P. J. Matts, J. Hadgraft and M. E. Lane, *Int. J. Pharm.*, 2013, **441**, 192–201.
6 Z. D. Draelos, K. Ertel and C. Berge, *Cutis*, 2005, **76**, 135–141.
7 P. Garidel, B. Fölting, I. Schaller and A. Kerth, *Biophys. Chem.*, 2010, **150**, 144–156.
8 P. M. Elias, *J. Invest. Dermatol.*, 2005, **125**, 183–200.
9 R. R. Ong and C. F. Goh, *Drug Delivery Transl. Res.*, 2024, **14**, 3512–3548.
10 J. S. Sohn and J.-S. Choi, *Saudi Pharm. J.*, 2023, **31**, 1229–1236.
11 Y. Oh, S. K. Bedingfield, S. T. Schneebeli, *et al.*, *npj Drug Discov.*, 2025, **2**, 23.
12 H. N. Jung, S.-Y. Lee, S. Lee, H. Youn and H.-J. Im, *Theranostics*, 2022, **12**, 7509–7531.
13 A. S. Alfutaimani, N. K. Alharbi, A. S. Alahmari, A. A. Alqabbani and A. M. Aldayel, *Int. J. Pharm.: X*, 2024, **8**, 100305.
14 W. Tiyaboonchai, P. Ngammuangman, S. Pan-On and D. T. Pham, *J. Appl. Pharm. Sci.*, 2025, **15**, 48–54.
15 F. J. S. U. Dewi, I. Kuncahyo and T. N. Saifullah, *Form. J. Multidiscip. Res.*, 2024, **3**, 3407–3426.
16 R. Basto, R. Andrade, C. Nunes, S. A. C. Lima and S. Reis, *Pharmaceutics*, 2021, **13**, 1968.
17 K. Yu, Y. Wang, T. Wan, Y. Zhai, S. Cao, W. Ruan, C. Wu and Y. Xu, *Int. J. Nanomed.*, 2018, **13**, 129–142.
18 Q. T. Nguyen, M. Noh, M. Song, J. Kim, S. Yang, U. T. Do, Q. S. Luu, Y. Park, J. Lee, J. Jang, N. Whiting, Y. I. Lee, J. B. Lee and Y. B. Lee, *ACS Appl. Mater. Interfaces*, 2025, **17**, 57976–57988, DOI: 10.1021/acsami.5c14268.
19 A.-G. Niculescu and A. M. Grumezescu, *Materials*, 2021, **14**, 6812.
20 S. Guo, Y. Li, H. Wang, Z. Yin and W. Wu, *Nanotechnol. Rev.*, 2019, **8**, 143–155.
21 R. Sheshala, C. A. Anuar, N. H. Abu Samah and M. Billa, *AAPS PharmSciTech*, 2019, **20**, 164.
22 B. Durakovic, *Period. Eng. Nat. Sci.*, 2018, **5**, 421–439.
23 T. Pyzdek, *The Six Sigma Handbook*, McGraw-Hill, New York, 2003.
24 S. N. Politis, P. Colombo, G. Colombo and D. M. Rekkas, *Drug Dev. Ind. Pharm.*, 2017, **43**, 889–901.
25 D. C. Montgomery, *Design and Analysis of Experiments*, Wiley, Hoboken, 2013.
26 K. Vanaja and R. H. S. Rani, *Clin. Res. Regul. Aff.*, 2007, **24**, 1–23.
27 M. Anderson and A. Omri, *Drug Delivery*, 2004, **11**, 33–39.
28 E. Abd, S. A. Yousef, M. N. Pastore, K. Telaprolu, Y. H. Mohammed, S. Namjoshi, J. E. Grice and M. S. Roberts, *Clin. Pharmacol.: Adv. Appl.*, 2016, **8**, 163–176.
29 R. S. Nair, N. Billa and A. P. Morris, *AAPS PharmSciTech*, 2025, **26**, 147, DOI: 10.1208/s12249-025-03143-2.
30 S. Dhoble and V. Patravale, *Drug Delivery Transl. Res.*, 2019, **9**, 980–996.
31 M. T. Luiz, J. S. R. Viegas, J. P. Abriata, F. Viegas, F. Testa Moura de Carvalho Vicentini, M. V. L. B. Bentley, M. Chorilli, J. M. Marchetti and D. R. Tapia-Blácido, *Eur. J. Pharm. Biopharm.*, 2021, **165**, 127–148.
32 Z. Németh, I. Csóka, R. Semnani Jazani, B. Sipos, H. Haspel, G. Kozma, Z. Kónya and D. G. Dobó, *Pharmaceutics*, 2022, **14**, 1798.
33 D.-Y. Wang, H. C. van der Mei, Y. Ren, H. J. Busscher and L. Shi, *Front. Chem.*, 2020, **7**, 872.
34 S. Bhattacharjee, *J. Controlled Release*, 2016, **235**, 337–351.
35 D. Khater, H. Nsairat, F. Odeh, M. Saleh, A. Jaber, W. Alshaer, A. A. Bawab and M. S. Mubarak, *Cosmetics*, 2021, **8**, 39.
36 I. D. L. Souza, V. Saez and C. R. E. Mansur, *Colloids Surf., B*, 2023, **230**, 113491.
37 E. Triantafyllopoulou, D. Selianitis, M. Chountoulesi, M. Karayianni, G. Valsami, S. Pispas and N. Pippa, *Adv. Colloid Interface Sci.*, 2026, **353**, 103884.
38 K. Somboon, C.-P. Chng, C. Huang and S. Gupta, *Int. J. Mol. Sci.*, 2025, **26**, 1555.
39 A. J. Guillot, M. Martínez Navarrete, T. M. Garrigues and A. Melero, *J. Controlled Release*, 2023, **355**, 624–654.
40 I. Katsogiannis, N. Naziris, A. Sarika, K. Gardikis, S. Hatziantoniou, N. Boukos, P. Dallas, N. Fikioris and C. Demetzos, *J. Drug Delivery Sci. Technol.*, 2024, **96**, 105654.
41 B. W. Barry, *Eur. J. Pharm. Sci.*, 2001, **14**, 101–114.
42 A. K. Chettupalli, S. P. N. Bukke, S. A. Rahaman, A. Unnisa, M. Adepu, M. Kavitha, M. R. Babu, M. R. Narapureddy and H. Onohuean, *Discover Appl. Sci.*, 2025, **7**, 58.
43 S.-I. Lee, S.-K. Nagayya-Sriraman, S. Shanmugam, R. Baskaran, C.-S. Yong, S.-K. Yoon, H.-G. Choi and B.-K. Yoo, *Biomol. Ther.*, 2011, **19**, 231–236.
44 L. Maione-Silva, E. G. de Castro, T. L. Nascimento, E. R. Cintra, L. C. Moreira, B. A. S. Cintra, M. C. Valadares and E. M. Lima, *Sci. Rep.*, 2019, **9**, 522.
45 J. Kaur, V. Mishra, S. K. Singh, M. Gulati, B. Kapoor, D. K. Chellappan, G. Gupta, H. Dureja, K. Anand, K. Dua, G. L. Khatik and K. Gowthamarajan, *J. Controlled Release*, 2021, **334**, 64–95.
46 Z. E. Jassim and N. A. Rajab, *Int. J. Pharm. Invest.*, 2025, **15**, 849–857.
47 M. Ghezzi, S. Pescina, C. Padula, P. Santi, E. Del Favero, L. Cantù and S. Nicoli, *J. Controlled Release*, 2021, **332**, 312–336.
48 Z. Zhang, P.-C. Tsai, T. Ramezanli and B. B. Michniak-Kohn, *Wiley Interdiscip. Rev.: Nanomed. Nanobiotechnol.*, 2013, **5**, 205–218.

49 S.-C. Wang, T.-C. Wei, W.-B. Chen and H.-K. Tsao, *J. Chem. Phys.*, 2004, **120**, 4980–4988.
50 D. Lombardo and M. A. Kiselev, *Pharmaceutics*, 2022, **14**, 543.
51 R. Silva, H. Ferreira, C. Little and A. Cavaco-Paulo, *Ultrason. Sonochem.*, 2010, **17**, 628–632.
52 W. Lin, R. Goldberg and J. Klein, *J. Mater. Chem. B*, 2022, **10**, 2820–2827.
53 J. W. Wiechers, C. L. Kelly, T. G. Blease and J. C. Dederen, *Int. J. Cosmet. Sci.*, 2004, **26**, 173–182.
54 S. Thomas, A. Bharti, K. Tharpa and A. Agarwal, *J. Pharm. Biomed. Anal.*, 2012, **60**, 86–90.